Draft version November 16, 2022
Typeset using LaTeX twocolumn style in AASTeX631

Dark matter particle properties from galaxy rotation curves and the theory of energy cascade

Zhijie (Jay) Xu [1]

[1] Physical and Computational Sciences Directorate
Pacific Northwest National Laboratory
Richland, WA 99354, USA

ABSTRACT

After years of null results in the search for dark matter, a different prospective might be required beyond the standard WIMP paradigm. We present a cascade theory to estimate dark matter particle mass, size, density, and many other properties. A comparison with the hydrodynamic turbulence is presented to reveal the unique features for the flow of dark matter. There exists an inverse mass and energy cascade from small to large scales to facilitate structure formation. A scale-independent rate of energy cascade $\varepsilon_u \approx -4.6 \times 10^{-7} m^2/s^3$ is identified. The energy cascade leads to a two-thirds law for pairwise velocity and a four-thirds law for halo core density and scale radius. Both scaling laws can be directly confirmed by N-body simulations and galaxy rotational curves. For the simplest case with only gravity involved and no viscosity, scaling laws can be extended down to the smallest scale, where quantum effects become important. Combining the rate of energy cascade ε_u, Planck constant $\hbar$, and gravitational constant G on the smallest scale, the mass of dark matter particles is found to be $0.9 \times 10^{12} GeV$ with a size around $3 \times 10^{-13} m$. Since the mass scale m_X is only weakly dependent on ε_u as $m_X \propto (-\varepsilon_u \hbar^5/G^4)^{1/9}$, the estimation of m_X should be pretty robust for a wide range of possible values of ε_u. If gravity is the only interaction and dark matter is fully collisionless, mass of $10^{12} GeV$ is required to produce the given rate of energy cascade ε_u. In other words, if mass has a different value, there must be some new interaction beyond gravity. This work suggests a heavy dark matter scenario produced in the early universe ($\sim 10^{-14} s$) with a mass much greater than WIMPs. Potential extension to self-interacting dark matter is also presented.

Keywords: Dark matter(353) — Galaxy rotation curves(619) — Astronomical simulations(1857)

1. INTRODUCTION

The existence of dark matter (DM) is supported by numerous astronomical observations. The most striking indications come from the dynamical motions of astronomical objects. The flat rotation curves of spiral galaxies point to the existence of galactic dark matter haloes with a total mass much greater than luminous matter (Rubin & Ford 1970; Rubin et al. 1980). The Planck measurements of the cosmic microwave background (CMB) anisotropies concludes that the amount of dark matter is about 5.3 times that of baryonic matter based on the standard ΛCDM cosmology (Aghanim et al. 2021).

Corresponding author: Zhijie (Jay) Xu
zhijie.xu@pnnl.gov

Though the nature of dark matter is still unclear, it is often assumed to be a thermal relic, weakly interacting massive particles (WIMPs) that were in local equilibrium in the early universe (Steigman & Turner 1985). These thermal relics freeze out as the reaction rate becomes comparable with the expansion of universe. The self-annihilation cross section required by the right DM abundance is on the same order as the typical electroweak cross section, in alignment with the supersymmetric extensions of the standard model ("WIMP miracle") (Jungman et al. 1996). The mass of thermal WIMPs ranges from a few GeV to hundreds GeV with the unitarity argument giving an upper bound of several hundred TeV (Griest & Kamionkowski 1990). However, no conclusive signals have been detected in either direct or indirect searches for thermal WIMPs in that range of mass. This hints that different thinking might be required beyond the standard WIMP paradigm.

This paper introduces a possible perspective that is based on fully understanding the flow behavior of dark matter on both large and small scales. Dark matter particle properties might be inferred by consistently extending the established laws for dark matter flow down to the smallest scales, below which the quantum effects become dominant. This extension follows a "top-down" approach. A classic example is the coupling of the virial theorem with Heisenberg's uncertainty principle for electrons,

$$\frac{e^2}{4\pi\varepsilon_0 r_e} = m_e v_e^2 \quad \text{and} \quad m_e v_e r_e = \hbar, \tag{1}$$

where ε_0 is the vacuum permittivity, $\hbar$ is the reduced Planck constant, e is the elementary charge, m_e is the electron mass, and r_e is the radius of orbit.

This coupling leads to the result for electron velocity v_e in the first circular orbit of Bohr atomic model. If Eq. (1) is unknown, by treating ε_0, e, and $\hbar$ as fundamental physical constants on the atomic scale, a simple dimensional analysis reveals the electron velocity $v_e \propto e^2/\varepsilon_0\hbar$. With Eq. (1), a more accurate result for v_e can be obtained along with the Sommerfeld's interpretation of the fine structure constant α (c is the speed of light),

$$v_e = \frac{e^2}{4\pi\varepsilon_0\hbar} \quad \text{and} \quad \alpha = \frac{v_e}{c} = \frac{e^2}{4\pi\varepsilon_0\hbar c} \approx \frac{1}{137}. \tag{2}$$

This example inspires some of our thinking to apply similar dimensional analysis and "top-down" approach for dark matter properties. However, dark matter is special. It is widely believed that dark matter is cold (non-relativistic), collisionless, dissipationless (optically dark), non-baryonic, and barely interacting with baryonic matter except through gravity. In addition, dark matter must be sufficiently smooth on large scales with a fluid-like behavior that is best described by a self-gravitating collisionless fluid dynamics (SG-CFD). A complete understanding of the nature of dark matter flow may provide key insights into the properties of dark matter particles.

At first glimpse, both SG-CFD and hydrodynamic turbulence contain the same essential ingredients, i.e. randomness, nonlinearity, and multiscale nature (Xu 2022a). This suggests a quick revisit of some fundamental ideas of turbulence, a long-standing unresolved problem in classical physics. Turbulence is ubiquitous in nature. In particular, homogeneous isotropic incompressible turbulence has been well-studied for many decades (Taylor 1935, 1938; de Karman & Howarth 1938; Batchelor 1953). Turbulence consists of a random collection of eddies (building blocks of turbulence) on different length scales that are interacting with each other and dynamically changing in space and time. The classical picture of turbulence is an eddy-mediated cascade process, where kinetic energy of large eddies feeds smaller eddies, which feeds even smaller eddies, and so on to the smallest scale η where viscous dissipation is dominant (see Fig. 1). The direct energy cascade can be best described by a poem (Richardson 1922):

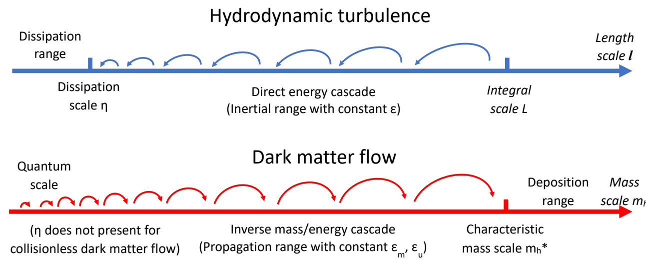

Figure 1. Schematic plot of the direct energy cascade in turbulence and the inverse mass and energy cascade in dark matter flow. Haloes merge with single mergers to facilitate a continuous mass and energy cascade to large scales. Scale-independent mass flux ε_m and energy flux ε_u are expected for haloes smaller than a characteristic mass scale (i.e. the propagation range corresponding to the inertial range for turbulence). Mass cascaded from small scales is consumed to grow haloes at scales above the characteristic mass (the deposition range similar to the dissipation range in turbulence), where mass and energy flux become scale-dependent.

"Big whirls have little whirls, That feed on their velocity;
And little whirls have lesser whirls, And so on to viscosity."

Provided the Reynolds number is high enough, there exists a range of length scales where the viscous force is negligible and the inertial force is dominant (inertial range). The rate ε (unit:m^2/s^3) of energy passing down the cascade is scale-independent in the inertial range and related to eddy velocity u and scale l as $\varepsilon \propto u^3/l$. This rate matches exactly the rate of energy dissipation due to viscosity ν on small scale. The inertial range extends down to the smallest (Kolmogorov) scale η, below which is the dissipation range (Fig. 1). The smallest length scale of inertial range $\eta = (\nu^3/\varepsilon)^{1/4}$ (shown in Fig. 1) is determined by ε and viscosity ν. While direct energy cascade is a dominant feature for 3D turbulence, there exists a range of scales over which energy is transferred from small to large length scales in 2D turbulence, i.e. an inverse energy cascade (Kraichnan 1967).

For the inertial range of turbulence with a constant energy flux ε, a universal form is established for the mth order longitudinal velocity structure function (Kolmogorov 1962) (or mth moments of the pairwise velocity in cosmology terms),

$$S_m^{lp}(r) = \left\langle \left(u_L^{'} - u_L\right)^m \right\rangle = \beta_m \varepsilon^{m/3} r^{m/3} \tag{3}$$

and for second order moment with m=2,

$$\begin{aligned} S_2^{lp}(r) &= \beta_2 \varepsilon^{2/3} r^{2/3} \\ \varepsilon &= \frac{(S_2^{lp}/\beta_2)^{3/2}}{r} = \frac{u^2}{r/u} = \frac{u^3}{r} \end{aligned} \tag{4}$$

with $\beta_2 \approx 2$ for m=2, where $u_L^{'}$ and u_L are two longitudinal velocities (see Fig. 3 for the definition) and r is the scale of separation. Here $u = (S_2^{lp}/\beta_2)^{1/2}$ is eddy's characteristic speed. Equation (4) describes the cascade of kinetic energy u^2 to smaller eddies in a typical turnaround time r/u. Does this simple scaling also apply to dark matter flow? how does this enhance our understanding of dark matter properties? These are the critical questions we will try to answer in this paper.

Flow of dark matter exhibits different behavior due to its collisionless and long-range interaction nature. First, the long-range gravity requires a broad spectrum of haloes to be formed to maximize the system entropy. Haloes facilitate an inverse mass cascade that is absent in hydrodynamic turbulence. The highly localized haloes are a major manifestation of nonlinear gravitational collapse (Neyman & Scott 1952; Cooray & Sheth 2002). As the building blocks of SG-CFD (counterpart to "eddies" in turbulence), the halo-mediated inverse mass cascade is a local, two-way, and asymmetric process in mass space. Haloes pass their mass onto larger and larger haloes, until halo mass growth becomes dominant over mass propagation. Consequently, there is a continuous cascade of mass from smaller to larger mass scales with a rate of mass transfer ε_m independent of mass scale in a certain range (propagation range in Fig. 1)). From this description, mass cascade can be described similarly with "eddies" (or "whirls") simply replaced by "haloes":

"Little haloes have big haloes, That feed on their mass; And big haloes have greater haloes, And so on to growth."

Second, both turbulence and dark matter flow are non-equilibrium systems that can never reach a final equilibrium. Both flows involve an constant energy cascade ε_u in certain range of scales. The mass/energy cascade is an intermediate statistically steady state for non-equilibrium systems to continuously maximize system entropy while evolving towards the limiting equilibrium. Both SG-CFD and 2D turbulence exhibit an inverse (kinetic) energy cascade, while 3D turbulence possesses a direct energy cascade (Fig. 1).

Finally, while viscous dissipation is the only mechanism to dissipate the kinetic energy in turbulence, it is not present in collisionless dark matter flow. Without a viscous force, there is no dissipation range in SG-CFD and the smallest length scale of inertial range is not limited by viscosity. This unique feature of dark matter flow enables us to extend the scale-independent constant ε_u down to the smallest scale, where quantum effects become important, if there are no other known interactions or forces involved except gravity. In addition, kinetic energy in collisionless dark matter flow cannot be dissipated without a viscous force. The linear increase of system kinetic energy with time can be used to estimate the constant rate of cascade ε_u (see Eq. (6)). In this paper, we will identify relevant physical laws and apply them for dark matter properties.

2. CONSTANT RATE OF ENERGY CASCADE

The basic dynamics of dark mater flow follows from the collisionless Boltzmann equations (CBE) (Mo et al. 2010). Alternatively, particle-based gravitational N-body simulations are widely used to study the dynamics of dark matter flow (Peebles 1980). The simulation data for this work was generated from N-body simulations carried out by the Virgo consortium. A comprehensive description of the simulation data can be found in (Frenk et al. 2000; Jenkins et al. 1998). The current work focuses on matter-dominant simulations with $\Omega_0 = 1$ and cosmological constant $\Lambda = 0$. This set of simulation data has been widely used in studies such as clustering statistics (Jenkins et al. 1998), the formation of halo clusters in large scale environments (Colberg et al. 1999), and testing models for halo abundance and mass functions (Sheth et al. 2001).

When a self-gravitating system in expanding background is concerned, the evolution of system energy can be described by a cosmic energy equation (Irvine 1961; Layzer 1963),

$$\frac{\partial E_y}{\partial t} + H(2K_p + P_y) = 0, \tag{5}$$

which is a manifestation of energy conservation in expanding background. Here K_p is the specific (peculiar) kinetic energy, P_y is the specific potential energy in physical coordinate, $E_y = K_p + P_y$ is the total energy, $H = \dot{a}/a$ is the Hubble parameter, a is the scale factor.

The cosmic energy equation (5) admits a linear solution of $K_p \propto t$ and $P_y \propto t$ (Fig. 2) such that a constant rate of energy cascade $\varepsilon_{\mathbf{u}}$ can be defined from $K_p = -\varepsilon_{\mathbf{u}} t$ or $P_y = 7\varepsilon_{\mathbf{u}} t/5$,

$$\varepsilon_u = -\frac{K_p}{t} = -\frac{3}{2}\frac{u^2}{t} = -\frac{3}{2}\frac{u_0^2}{t_0} \approx -4.6 \times 10^{-7} \frac{m^2}{s^3}, \tag{6}$$

where $u_0 \equiv u(t = t_0) \approx 354.6 km/s$ is the one-dimensional velocity dispersion of dark matter particles from simulation, and t_0 is the physical time at present

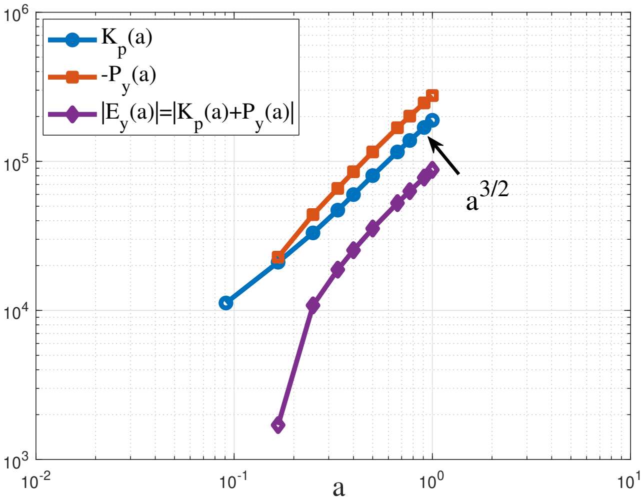

Figure 2. The time variation of specific kinetic and potential energies from N-body simulation. Both exhibit power-law scaling with scale factor a, i.e. $K_p(a) \propto a^{3/2} \propto t$ and $P_y(a) \propto a^{3/2} \propto t$. The proportional constant $\varepsilon_{\mathbf{u}}$ can be estimated in Eq. (6).

epoch. The constant $\varepsilon_{\mathbf{u}}$ has a physical meaning as the rate of energy cascade across different scales that is facilitated by the inverse mass cascade. The existence of a negative $\varepsilon_{\mathbf{u}} < 0$ reflects the inverse cascade from small to large scales that can be confirmed by galaxy rotation curves (Fig. 8).

3. TWO-THIRDS LAW FROM SIMULATION

Different types of statistical measures are traditionally used to characterize the turbulent flow, i.e. the correlation functions, structure functions, and power spectrum. In this paper, we focus on the structure functions that describe how energy is distributed and transferred across different length scales. In N-body simulations, for a pair of particles at locations $\mathbf{x}$ and $\mathbf{x}'$ with velocity $\mathbf{u}$ and $\mathbf{u}'$, the second order longitudinal structure function S_2^{lp} (pairwise velocity dispersion in cosmology terms) reads

$$S_2^{lp}(r,a) = \left\langle (\Delta u_L)^2 \right\rangle = \left\langle \left(u_L' - u_L\right)^2 \right\rangle, \qquad (7)$$

where $u_L = \mathbf{u} \cdot \hat{\mathbf{r}}$ and $u_L' = \mathbf{u}' \cdot \hat{\mathbf{r}}$ are two longitudinal velocities. The distance $r \equiv |\mathbf{r}| = |\mathbf{x}' - \mathbf{x}|$ and the unit vector $\hat{\mathbf{r}} = \mathbf{r}/r$ (see Fig. 3).

For a given scale r, all particle pairs with the same separation r can be identified from the simulation. The particle position and velocity data were recorded to compute the structure function in Eq. (7) by averaging that quantity over all pairs with the same separation r (pairwise average). Figure 4 presents the variation of S_2^{lp} with scale r at different redshift $z = 1/a - 1$, while Figure 5 plots the variation of $\langle u_L^2 \rangle$ (the variance of u_L)

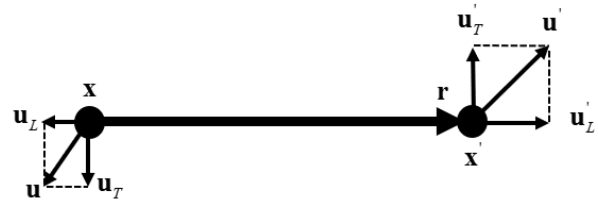

Figure 3. Sketch of longitudinal and transverse velocities, where $\mathbf{u}_T$ and $\mathbf{u}_T'$ are transverse velocities at two locations $\mathbf{x}$ and $\mathbf{x}'$. u_L and u_L' are two longitudinal velocities.

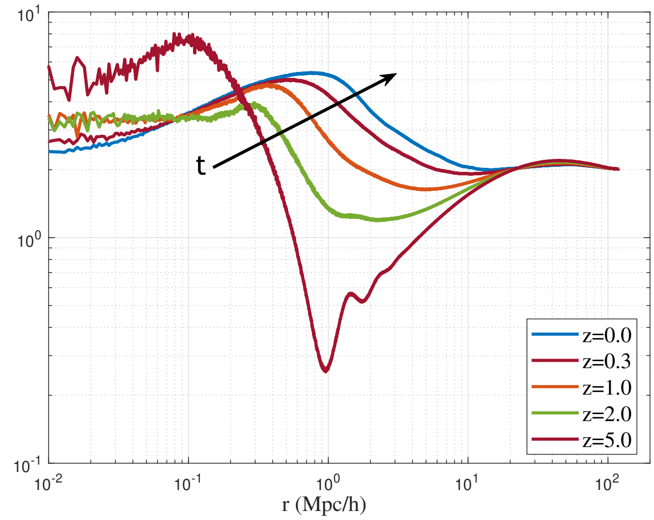

Figure 4. The variation of second order longitudinal structure function with scale r and redshift z. The structure function S_2^{lp} (pairwise velocity dispersion) is normalized by velocity dispersion u^2. Two limits $\lim_{r\to 0} S_2^{lp} = \lim_{r\to\infty} S_2^{lp} = 2u^2$ can be identified on small and large scales.

with scale r. There exist limits $\lim_{r\to 0} S_2^{lp} = \lim_{r\to\infty} S_2^{lp} = 2u^2$ because the correlation coefficient ρ_L between u_L and u_L' has a limit $\lim_{r\to 0} \rho_L = 1/2$ on small scale and $\lim_{r\to\infty} \rho_L = 0$ on large scale. Therefore, we should have (see Fig. 5)

$$\begin{gathered}\lim_{r\to 0} \left\langle u_L^2 \right\rangle = \lim_{r\to 0} \left\langle u_L'^2 \right\rangle = 2\lim_{r\to 0} \left\langle u_L u_L' \right\rangle = 2u^2 \\ \text{and} \\ \lim_{r\to\infty} \left\langle u_L^2 \right\rangle = \lim_{r\to\infty} \left\langle u_L'^2 \right\rangle = u^2,\end{gathered} \qquad (8)$$

where $\lim_{r\to 0} \langle u_L u_L' \rangle = \lim_{r\to 0} \rho_L \langle u_L^2 \rangle = u^2$. By contrast, $\langle u_L^2 \rangle = u^2$ on all scales for incompressible hydrodynamic turbulence.

The original scaling law for incompressible flow postulates that $S_2^{lp} \propto \varepsilon^{2/3} r^{2/3}$ in the inertial range (Eq. (4)), where the effect of viscosity is negligible in inertial range (Kolmogoroff 1941). Here ε is the rate of energy dissipation for direct energy cascade from large to small length

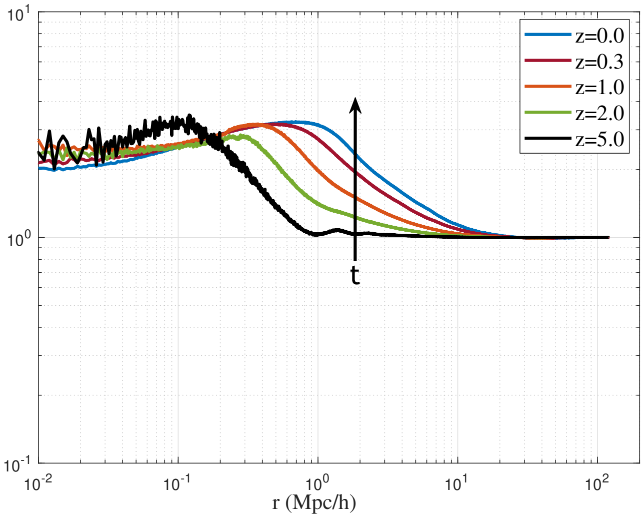

Figure 5. The variation of longitudinal velocity dispersion with scale r and redshift z. The longitudinal dispersion $\langle u_L^2 \rangle$ is normalized by velocity dispersion u^2 of entire system. Two limits $\lim_{r\to 0}\langle u_L^2 \rangle = 2u^2$ and $\lim_{r\to\infty}\langle u_L^2 \rangle = u^2$ can be identified on small and large scales. By contrast, $\langle u_L^2 \rangle = u^2$ on all scales for incompressible hydrodynamic turbulence.

sales in Fig. 1. Figure 4 clearly tells us that the original scaling law in Eq. (3) is not valid for dark matter flow due to its collisionless nature. However, a new scaling law can be established (two-thirds law in Eq. (9)).

First, halo cores should be incompressible due to the stable clustering hypothesis, i.e. no net stream motion in proper coordinate along halo radial direction such that the proper velocity of dark matter is incompressible on small scales. This prediction hints to a similar scaling law might exist for dark matter flow. Second, just like the hydrodynamic turbulence, energy cascade with a constant rate ε_u also exists in dark matter flow, but in an opposite direction. Therefore, it would be reasonable to expect the second order structure function S_2^{lp} is related to ε_u in some way, but different from Eq. (4).

In hydrodynamic turbulence, the structure function $\lim_{r\to 0} S_2^{lp} = 0$ with $\lim_{r\to 0}\rho_L = 1$ because of the viscous force. However, in dark matter flow, the small-scale limit $\lim_{r\to 0} S_2^{lp} = 2u^2 \neq 0$ due to the collisionless nature (Fig. 4). Instead, a reduced structure function $S_{2r}^{lp} = S_2^{lp} - 2u^2$ can be constructed with the same limit $\lim_{r\to 0} S_{2r}^{lp} = 0$ as that in turbulence. This is a simple "renormalization" to deal with the non-vanishing pairwise velocity dispersion at $r = 0$ in collisionless system.

Pair of particles with a small separation r is more likely from the same halo (two particles in the same halo), while different pairs can be from different haloes of different size (see Fig. 6). The original pairwise dispersion S_2^{lp} represents the total kinetic energy of par-

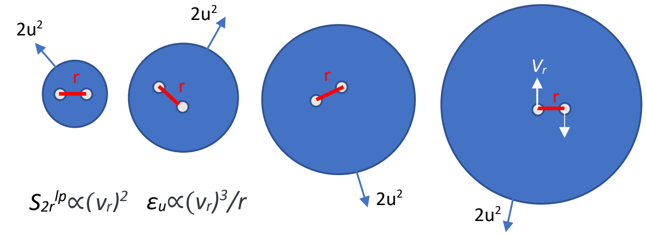

Figure 6. On small scale r, pair of particles is likely from the same halo. Different pairs can be from haloes of different size. The kinetic energy of entire halo ($2u^2$) is relatively independent of halo mass. The reduced structure function $S_{2r}^{lp} = S_2^{lp} - 2u^2$ represents the portion of kinetic energy (v_r^2) that is cascaded across scales with a constant rate ε_u.

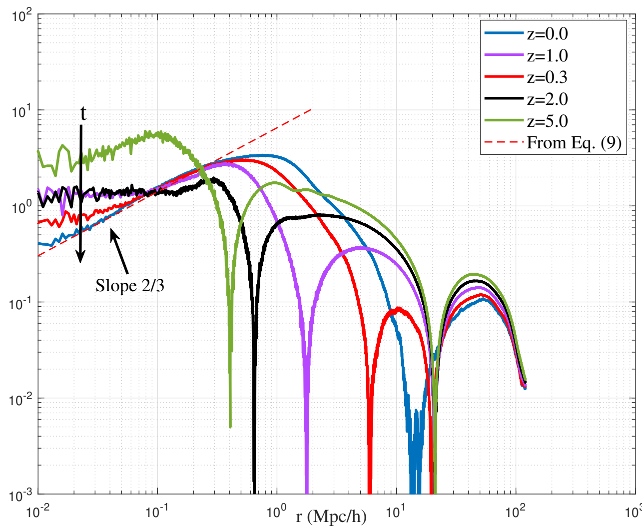

Figure 7. The variation of reduced structure function with scale r and redshift z. Structure function is normalized by velocity dispersion u^2. A two-thirds law $S_{2r}^{lp} \propto (-\varepsilon_u)^{2/3} r^{2/3}$ can be identified on small scale below a length scale $r_l = -u_0^3/\varepsilon_u$, when inverse energy cascade is established with a constant energy flux $\varepsilon_u < 0$. The model from Eq. (9) is also presented for comparison.

ticle pairs on scale r including the kinetic energy both from the relative motion of particle pairs and from the halo that particle pair resides in. The reduced structure function $S_{2r}^{lp} = S_2^{lp} - 2u^2$ represents only the kinetic energy v_r^2 from the relative motion of two particles. This description indicates that S_{2r}^{lp} should be determined by and only by ε_u (unit: m^2/s^3), scale r, and gravitational constant G. By a simple dimensional analysis, the reduced structure function S_{2r}^{lp} must follow a two-thirds law for small r, i.e. $S_{2r}^{lp} \propto v_r^2 \propto (-\varepsilon_u)^{2/3} r^{2/3}$.

Figure 7 plots the variation of reduced structure function S_{2r}^{lp} with scale r at different redshifts z from N-body simulation. The range with $S_{2r}^{lp} \propto r^{2/3}$ can be clearly identified below a length scale $r_l = -u_0^3/\varepsilon_u$.

This range is formed along with the formation of haloes and the establishment of inverse energy cascade. As expected, the reduced structure function quickly converges to $S_{2r}^{lp} \propto (-\varepsilon_u)^{2/3} r^{2/3}$ with time. The second order reduced longitudinal structure function on small scale now reads (normalized by $a^{3/2} \propto t$)

$$S_{2r}^{lp}(r)/a^{3/2} = \beta_2^* (-\varepsilon_u)^{2/3} r^{2/3} \propto v_r^2. \tag{9}$$

The length scale r_l (size of the largest halo in propagation range) is determined by u_0 and ε_u (see Fig. 8)

$$r_l = -\frac{u_0^3}{\varepsilon_u} = \frac{4}{9}\frac{u_0}{H_0} = \frac{2}{3}u_0 t_0 \approx 1.57 Mpc/h. \tag{10}$$

The proportional constant $\beta_2^* \approx 9.5$ can be found from Fig. 7, where model (9) is also presented for comparison.

The higher order structure functions can be similarly studied. We can demonstrate that all even order reduced structure functions in Eq. (7) follow the two-thirds law $\langle (\Delta u_L)^{2n} \rangle \propto r^{2/3}$, while odd order structure functions $\langle (\Delta u_L)^{2n+1} \rangle \propto r$ on small scale. Results for high order structure functions are completely different from that of hydrodynamic turbulence in Eq. (3).

4. FOUR-THIRDS LAW FROM ROTATION CURVES

The two-thirds law on small scale (Eq. (9)) is validated by N-body simulations in Fig. 7. Now we will look for observational evidence of energy cascade and universal scaling laws. The two-thirds law can be equivalently written as (see Eq. (9))

$$\left(2v_r^2/r\right) v_r = 2v_r^2/\left(r/v_r\right) = \left(-\lambda_u \varepsilon_u\right), \tag{11}$$

where λ_u is just a dimensionless numerical constant on the order of unity. Equation (11) describes the cascade of kinetic energy with a constant rate ε_u in halo core region ($r \leq r_s$, where r_s is the halo scale radius). The kinetic energy v_r^2 on scale r is cascaded to large scale during a turnaround time of $t_r = r/v_r$, with both v_r^2 and halo size r_s increasing with time.

Combining Eq. (11) with the virial theorem $Gm_r/r \propto v_r^2$ on scale r, we can easily obtain the mass scale m_r (mass enclosed within r), density scale ρ_r (mean halo density enclosed within r), velocity scale v_r (circular velocity at r), and time t_r, all determined by constants ε_u, G, and the scale r:

$$\begin{aligned} &m_r = \alpha_r \varepsilon_u^{2/3} G^{-1} r^{5/3} \quad , \quad \rho_r = \beta_r \varepsilon_u^{2/3} G^{-1} r^{-4/3}, \\ &v_r \propto (-\varepsilon_u r)^{1/3} \quad , \quad t_r \propto (-\varepsilon_u)^{-1/3} r^{2/3}, \end{aligned} \tag{12}$$

where α_r and β_r are two numerical constants. Among these universal scaling laws, the four-thirds law $\rho_r(r) \propto$

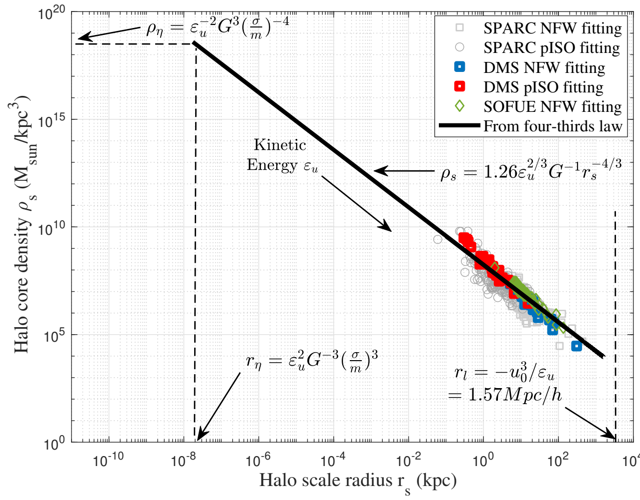

Figure 8. The four-thirds law compared against actual data from galaxy rotation curves. Good agreement confirms the existence of inverse energy cascade with a constant rate ε_u. The self-interacting dark matter model with a cross-section σ/m leads to the smallest structure with a size r_η and a maximum density ρ_η determined by ε_u, G, and σ/m (Table 1), below which no coherent structure can exist. The largest scale r_l is determined by the dispersion u_0 and ε_u (Eq. (10)).

$r^{-4/3}$ for mean mass density enclosed with scale r can be directly compared against the data from galaxy rotation curves (see Fig. 8).

Important information for dark matter haloes can be extracted from galaxy rotation curves by decomposing them into contributions from different mass components. Once the halo density model is selected, the scale radius r_s and mean density ρ_s within r_s can be rigorously obtained by fitting to the decomposed rotation curve. In this work, for pseudo-isothermal (pISO) (Adams et al. 2014) and NFW density models (Navarro et al. 1997), three sources of galaxy rotation curves are used to extract r_s and ρ_s,

1. SPARC (Spitzer Photometry & Accurate Rotation Curves) including 175 late-type galaxies (Lelli et al. 2016; Li et al. 2020);

2. DMS (DiskMass Survey) including 30 spiral galaxies (Martinsson et al. 2013);

3. SOFUE (compiled by Sofue) with 43 galaxies (Sofue 2016).

Figure 8 presents the variation of halo core density ρ_s with scale r_s obtained from rotation curves (symbols). The four-thirds law (Eq. (12)) is also plotted (thick line) with constants $\beta_r = 1.26$ or $\alpha_r = 5.28$ obtained from these data. From this figure, dark matter haloes follow the four-thirds law across six orders with a tight scatter.

This plot, again, confirms the existence of a constant rate of cascade ε_u for haloes with $r_s < r_l$. The scatter of data might be because of the spatial intermittence of ε_u that is dependent on local environment.

5. DARK MATTER PARTICLE PROPERTIES

Since viscosity is absent in fully collisionless dark matter flow, the scale-independent constant rate of energy cascade ε_u in Eq. (6) should extend down to the smallest scale where quantum effects become important. Assuming gravity is the only interaction between unknown dark matter particles (traditionally denoted by $\boldsymbol{X}$), the dominant physical constants on that scale are the (reduced) Planck constant $\hbar$, the gravitational constant G, and the rate of energy cascade ε_u. Other physical quantities can be easily found by a simple dimensional analysis (similar to the electron example in Eq. (2)). Two examples are the critical mass and length scales,

$$m_X = \left(-\varepsilon_u \hbar^5/G^4\right)^{\frac{1}{9}} \tag{13}$$

and

$$l_X = \left(-G\hbar/\varepsilon_u\right)^{\frac{1}{3}}. \tag{14}$$

The two-thirds law (or the four-thirds law) identified in dark matter flow (Fig. 7) should also extend down to the smallest length scale if only gravity is present without any other known interactions. Just like the "top-down" approach for electron example coupling the virial theorem with uncertainty principle in Eq. (1), a refined treatment to couple relevant laws on the smallest scale may offer more complete solutions than a simple dimensional analysis. Let's consider two $\boldsymbol{X}$ particles on the smallest scale with a separation $r = l_X$ in the rest frame of center of mass. We have

$$m_X V_X \cdot l_X/2 = \hbar, \tag{15}$$

$$2V_X^3/l_X = a_X \cdot v_X = -\lambda_u \varepsilon_u, \tag{16}$$

$$G m_X/l_X = 2V_X^2, \tag{17}$$

where Eq. (15) is from the uncertainty principle for momentum and position if $\boldsymbol{X}$ particles exhibit the wave-particle duality. Equation (16) is the "uncertainty" principle for particle acceleration and velocity due to scale-independent energy flux ε_u, which is also the two-thirds law in Eq. (11). The last Eq. (17) is from the virial theorem for potential and kinetic energy.

Finally, with the following values for three constants

$$\begin{aligned}
&\varepsilon_u = -4.6 \times 10^{-7} m^2/s^3,\\
&\hbar = 1.05 \times 10^{-34} kg \cdot m^2/s,\\
&G = 6.67 \times 10^{-11} m^3/\left(kg \cdot s^2\right),
\end{aligned} \tag{18}$$

complete solutions of Eqs. (15)-(17) are ($\lambda_u = 1$)

$$\begin{aligned}
l_X &= \left(-\frac{2G\hbar}{\lambda_u \varepsilon_u}\right)^{\frac{1}{3}} = 3.12 \times 10^{-13} m,\\
t_X &= \frac{l_X}{V_X} = \left(-\frac{32G^2\hbar^2}{\lambda_u^5 \varepsilon_u^5}\right)^{\frac{1}{9}} = 7.51 \times 10^{-7} s,
\end{aligned} \tag{19}$$

$$\begin{aligned}
m_X = \left(-\frac{256\lambda_u \varepsilon_u \hbar^5}{G^4}\right)^{\frac{1}{9}} &= 1.62 \times 10^{-15} kg\\
&= 0.90 \times 10^{12} GeV,
\end{aligned} \tag{20}$$

$$\begin{aligned}
V_X &= \left(\frac{\lambda_u^2 \varepsilon_u^2 \hbar G}{4}\right)^{\frac{1}{9}} = 4.16 \times 10^{-7} m/s,\\
a_X &= \left(-\frac{4\lambda_u^7 \varepsilon_u^7}{\hbar G}\right)^{\frac{1}{9}} = 1.11 m/s^2.
\end{aligned} \tag{21}$$

The time scale t_X is close to the characteristic time for weak interactions ($10^{-6} \sim 10^{-10} s$), while the length scale l_X is greater than the characteristic range of strong interaction ($\sim 10^{-15} m$) and weak interaction ($\sim 10^{-18} m$). By assuming a scale-independent rate of energy cascade ε_u down to the smallest scale, we can determine all relevant properties for dark matter particles.

The "thermally averaged cross section" of $\boldsymbol{X}$ particle is around $l_X^2 V_X = 4 \times 10^{-32} m^3/s$. This is on the same order as the cross section required for the correct abundance of today via a thermal production ("WIMP miracle"), where $\langle \sigma v \rangle \approx 3 \times 10^{-32} m^3 s^{-1}$. The "cross section σ/m" for $\boldsymbol{X}$ particle is around $l_X^2/m_X = 6 \times 10^{-11} m^2/kg$, which is effectively collisionless.

In addition, a new constant μ_X can be introduced,

$$\begin{aligned}
\mu_X &= m_X a_X \cdot V_X = F_X \cdot V_X = -m_X \varepsilon_u\\
&= \left(-\frac{256\varepsilon_u^{10}\hbar^5}{G^4}\right)^{\frac{1}{9}} = 7.44 \times 10^{-22} kg \cdot m^2/s^3
\end{aligned} \tag{22}$$

which is a different representation of ε_u. In other words, the fundamental physical constants on the smallest scale can be $\hbar$, G, and the power constant μ_X. An energy scale is set by $\mu_X t_X/4 = \hbar/t_X = \sqrt{\hbar\mu_X}/2 = 0.87 \times 10^{-9} eV$ for the possible dark matter annihilation or decay, much smaller than the Rydberg energy (the ionization energy of hydrogen atom) of 13.6 eV.

Finally, a quantum interpretation for Eqs. (16) or (22), if any, should be very insightful. The relevant mass density is around $m_X/l_X^3 \approx 5.33 \times 10^{22} kg/m^3$, much larger than the nuclear density that is on the order of $10^{17} kg/m^3$. The pressure scale

$$P_X = \frac{m_X a_X}{l_X^2} = \frac{8\hbar^2}{m_X}\rho_{nX}^{5/3} = 1.84 \times 10^{10} P_a \tag{23}$$

sets the highest pressure or the possible "degeneracy" pressure of dark matter that stops further gravitational collapse. Equation (23) is an analogue of the degeneracy pressure of ideal Fermi gas, where $\rho_{nX} = l_X^{-3}$ is the particle number density.

With today's dark matter density around $2.2 \times 10^{-27} kg/m^3$ and local density $7.2 \times 10^{-22} kg/m^3$, the mean separation between $\boldsymbol{X}$ particles is about $l_u \approx 10^4 m$ in entire universe and $l_c \approx 130m$ locally. If universe is always matter dominant, $\boldsymbol{X}$ particle should be produced at a time t_p same as $t_X \sim 10^{-7}s$ in Eq. (19) because the period of haloes approximates the time that halo is formed. A better estimation is to use the scale factor $a_p = l_X/l_u \approx 3 \times 10^{-17}$ to estimate the time $t_p \approx a_p^2/(2H_0\sqrt{\Omega_{rad}}) = 2 \times 10^{-14}s$ with radiation fraction $\Omega_{rad} \approx 10^{-4}$ (radiation dominant). This points to an early production of $\boldsymbol{X}$ particles during inflationary and electroweak epoch.

The mass scale we predict is around $0.9 \times 10^{12} GeV$ (Eq. (20)). This is well beyond the mass range of standard thermal WIMPs, but in the range of nonthermal relics, the so-called super heavy dark matter (SHDM). Our prediction is not dependent on the exact production mechanism of dark matter. One example mechanism can be the gravitational particle production in quintessential inflation (Ford 1987; Haro & Saló 2019; Peebles & Vilenkin 1999). The nonthermal relics from gravitational production do not have to be in the local equilibrium in early universe or obey the unitarity bounds for thermal WIMPs. To have the right abundance generated during inflation, these nonthermal relics should have a mass range between 10^{12} and 10^{13} GeV (Chung et al. 1999; Kolb & Long 2017). The other possible superheavy dark mater candidate is the crypton in string or M theory with a mass around 10^{12}Gev to give the right abundance (Ellis et al. 1990; Benakli et al. 1999). Our prediction of dark matter particle mass seems in good agreement with both theories. Potential direct and indirect detection of ultra-heavy dark matter was also discussed in the literature (Carney et al. 2022; Blanco et al. 2022).

To have the right abundance of dark matter at the present epoch, SHDM must be stable with a lifetime much greater than the age of universe. In the first scenario, if $\boldsymbol{X}$ particles directly decay or annihilate into standard model particles, the products could be detected indirectly. The decay of SHDM particles could be the source of ultra-high energy cosmic rays (UHECR) above the Greisen-Zatzepin-Kuzmin cut-off (Greisen 1966). Constraints on the mass and lifetime of SHDM can be obtained from the absence of ultra-high-energy photons and cosmic ray (Anchordoqui et al. 2021). For a given mass scale of $10^{12}GeV$, the lifetime is expected to be $\tau_X \geq 5 \times 10^{22} yr$. In addition, if instantons are responsible for the decay, lifetime can be estimated by (Anchordoqui et al. 2021)

$$\tau_X \approx \frac{\hbar e^{1/\alpha_X}}{m_X c^2}, \tag{24}$$

where α_X is a coupling constant on the scale of the interaction considered. With the lifetime $\tau_X \geq 5 \times 10^{22} yr$, the coupling constant should satisfy $\alpha_X \leq 1/152.8$ from Eq. (24).

For comparison, a different (second) scenario can be proposed. There can be a slow decay for $\boldsymbol{X}$ particle with an energy on the order of $\hbar/t_X$. In this slow decay scenario, the lifetime it takes for a complete decay of a single $\boldsymbol{X}$ particle can be estimated as,

$$\tau_X = \frac{m_X c^2}{\mu_X} = -\frac{c^2}{\varepsilon_u} \approx \frac{\hbar e^{1/\alpha_X}}{m_X c^2}, \tag{25}$$

where $\tau_X \approx 2 \times 10^{23} s = 6.2 \times 10^{15} yr$ is also much greater than the age of our universe, but shorter than the lifetime in the first scenario. The coupling constant is estimated as $\alpha_X \approx 1/136.85$.

6. SELF-INTERACTING DARK MATTER

Note that the mass scale m_X is only weakly dependent on ε_u as $m_X \propto \varepsilon_u^{1/9}$ (Eq. (20)) such that the estimation of m_X should be pretty robust for a wide range of possible values of ε_u. A small change in m_X requires huge change in ε_u. Unless gravity is not the only interaction, the uncertainty in predicted m_X should be small. In other words, if our estimation of ε_u (Eq. (6)) is accurate and gravity is the only interaction on the smallest scale, it seems not possible for dark matter particle with any mass far below 10^{12}GeV to produce the given rate of energy cascade ε_u. If mass has a different value, there must be some new interaction beyond gravity. This can be the self-interacting dark matter (SIDM) model proposed as a potential solution for "cusp-core" problem (Spergel & Steinhardt 2000).

For self-interacting dark matter, a key parameter is the cross section σ/m (in unit: m^2/kg) of self-interaction that can be constrained by various astrophysical observations. Self-interaction introduces an additional scale, below which the self-interaction is dominant over gravity to suppress all small-scale structures and two-thirds law is no longer valid. In this case, the dark matter particle properties can be obtained only if the nature and dominant constants of self-interaction is known. The lowest scale for two-thirds law is related to three constants in principle, i.e. the rate of energy cascade ε_u, the gravitational constant G, and the cross section σ/m. In other words, the cross section might be estimated if the scale of the smallest structure is known.

Table 1. Physical scales for the flow of dark matter

Scales	Fully collisionless	Self-interacting
Length	$l_X = (-2G\hbar/\varepsilon_u)^{1/3}$	$r_\eta = \varepsilon_u^2 G^{-3}(\sigma/m)^3$
Time	$t_X = \left(-32G^2\hbar^2/\varepsilon_u^5\right)^{1/9}$	$t_\eta = \varepsilon_u G^{-2}(\sigma/m)^2$
Mass	$m_X = \left(-256\varepsilon_u\hbar^5/G^4\right)^{1/9}$	$m_\eta = \varepsilon_u^4 G^{-6}(\sigma/m)^5$
Density	$\rho_X = \left(\varepsilon_u^{10}\hbar^{-4}/G^{13}\right)^{1/9}$	$\rho_\eta = \varepsilon_u^{-2} G^3(\sigma/m)^{-4}$

Taking the value of $\sigma/m = 0.01m^2/kg$ used for cosmological SIDM simulation to reproduce the right halo core size and central density (Rocha et al. 2013), Table 1 lists the relevant quantities on the smallest scale for both collisionless and self-interacting dark matter (also plotted in Fig. 8). More insights can be obtained by extending the current statistical analysis to self-interacting dark matter flow simulations.

7. CONCLUSIONS

The theory of energy cascade is proposed for dark matter flow to identify dark matter properties. The energy cascade leads to a two-thirds law for pairwise velocity or a four-thirds law for halo core density and scale radius. Both can be confirmed by N-body simulations and galaxy rotation curves. Since viscosity is not present and if gravity is the only interaction, established scaling laws can be extended to the smallest scale, where quantum effects become important. The dominant constants on that scale include a constant rate of energy cascade ε_u, the Planck constant $\hbar$, and gravitational constant G. Applying the dimensional analysis or the "top-down" approach, dark matter particles are found to have a mass around $0.9\times10^{12}GeV$ and a size around $3.12\times10^{-13}m$, along with many other important properties postulated. Potential extension to self-interacting dark matter is also discussed with relevant scales estimated for given cross section σ/m.

DATA AVAILABILITY

Two datasets for this article, i.e. a halo-based and correlation-based statistics of dark matter flow, are available on Zenodo (Xu 2022b,c), along with the accompanying presentation "A comparative study of dark matter flow & hydrodynamic turbulence and its applications" (Xu 2022a). All data are also available on GitHub (Xu 2022d).

REFERENCES

Adams, J. J., Simon, J. D., Fabricius, M. H., et al. 2014, ApJ, 789, 63, doi: 10.1088/0004-637X/789/1/63

Aghanim, N., Akrami, Y., Ashdown, M., et al. 2021, Astronomy & Astrophysics, 652, doi: 10.1051/0004-6361/201833910

Anchordoqui, L. A., Berat, C., Bertaina, M. E., et al. 2021, Astroparticle Physics, 132, doi: 10.1016/j.astropartphys.2021.102614

Batchelor, G. K. 1953, The Theory of Homogeneous Turbulence (Cambridge, UK: Cambridge University Press)

Benakli, K., Ellis, J., & Nanopoulos, D. V. 1999, PhRvD, 59, 047301, doi: 10.1103/PhysRevD.59.047301

Blanco, C., Elshimy, B., Lang, R. F., & Orlando, R. 2022, Physical Review D, 105, doi: 10.1103/physrevd.105.115031

Carney, D., Raj, N., Bai, Y., et al. 2022, Snowmass2021 Cosmic Frontier White Paper: Ultraheavy particle dark matter, arXiv, doi: 10.48550/ARXIV.2203.06508

Chung, D. J. H., Kolb, E. W., & Riotto, A. 1999, Physical Review D, 59, doi: 10.1103/PhysRevD.59.023501

Colberg, J. M., White, S. D. M., Jenkins, A., & Pearce, F. R. 1999, Monthly Notices of the Royal Astronomical Society, 308, 593, doi: 10.1046/j.1365-8711.1999.02400.x

Cooray, A., & Sheth, R. 2002, Physics Reports-Review Section of Physics Letters, 372, 1, doi: 10.1016/S0370-1573(02)00276-4

de Karman, T., & Howarth, L. 1938, Proceedings of the Royal Society of London Series a-Mathematical and Physical Sciences, 164, 0192, doi: 10.1098/rspa.1938.0013

Ellis, J., Lopez, J. L., & Nanopoulos, D. V. 1990, Physics Letters B, 247, 257, doi: 10.1016/0370-2693(90)90893-B

Ford, L. H. 1987, Phys. Rev. D, 35, 2955, doi: 10.1103/PhysRevD.35.2955

Frenk, C. S., Colberg, J. M., Couchman, H. M. P., et al. 2000, arXiv:astro-ph/0007362v1, doi: 10.48550/arXiv.astro-ph/0007362

Greisen, K. 1966, Phys. Rev. Lett., 16, 748, doi: 10.1103/PhysRevLett.16.748

Griest, K., & Kamionkowski, M. 1990, Physical Review Letters, 64, 615, doi: 10.1103/PhysRevLett.64.615

Haro, J., & Saló, L. A. 2019, Phys. Rev. D, 100, 043519, doi: 10.1103/PhysRevD.100.043519

Irvine, W. M. 1961, Thesis, HARVARD UNIVERSITY

Jenkins, A., Frenk, C. S., Pearce, F. R., et al. 1998, Astrophysical Journal, 499, 20, doi: 10.1086/305615

Jungman, G., Kamionkowski, M., & Griest, K. 1996, Physics Reports-Review Section of Physics Letters, 267, 195, doi: 10.1016/0370-1573(95)00058-5

Kolb, E. W., & Long, A. J. 2017, Physical Review D, 96, doi: 10.1103/PhysRevD.96.103540

Kolmogoroff, A. N. 1941, Comptes Rendus De L Academie Des Sciences De L Urss, 32, 16. ⟨GotoISI⟩://WOS:000201918500005

Kolmogorov, A. N. 1962, Journal of Fluid Mechanics, 13, 82, doi: 10.1017/S0022112062000518

Kraichnan, R. H. 1967, Physics of Fluids, 10, 1417, doi: 10.1063/1.1762301

Layzer, D. 1963, Astrophysical Journal, 138, 174, doi: 10.1086/147625

Lelli, F., McGaugh, S. S., & Schombert, J. M. 2016, AJ, 152, 157, doi: 10.3847/0004-6256/152/6/157

Li, P., Lelli, F., McGaugh, S., & Schombert, J. 2020, ApJS, 247, 31, doi: 10.3847/1538-4365/ab700e

Martinsson, T. P. K., Verheijen, M. A. W., Westfall, K. B., et al. 2013, A&A, 557, A131, doi: 10.1051/0004-6361/201321390

Mo, H., van den Bosch, F., & White, S. 2010, Galaxy formation and evolution (Cambridge: Cambridge University Press)

Navarro, J. F., Frenk, C. S., & White, S. D. M. 1997, Astrophysical Journal, 490, 493, doi: 10.1086/304888

Neyman, J., & Scott, E. L. 1952, Astrophysical Journal, 116, 144, doi: 10.1086/145599

Peebles, P. J. E. 1980, The Large-Scale Structure of the Universe (Princeton, NJ: Princeton University Press)

Peebles, P. J. E., & Vilenkin, A. 1999, Phys. Rev. D, 59, 063505, doi: 10.1103/PhysRevD.59.063505

Richardson, L. F. 1922, Weather Prediction by Numerical Process (Cambridge, UK: Cambridge University Press)

Rocha, M., Peter, A. H. G., Bullock, J. S., et al. 2013, Monthly Notices of the Royal Astronomical Society, 430, 81, doi: 10.1093/mnras/sts514

Rubin, V. C., & Ford, W. K. 1970, Astrophysical Journal, 159, 379, doi: 10.1086/150317

Rubin, V. C., Ford, W. K., & Thonnard, N. 1980, Astrophysical Journal, 238, 471, doi: 10.1086/158003

Sheth, R. K., Mo, H. J., & Tormen, G. 2001, Monthly Notices of the Royal Astronomical Society, 323, 1, doi: 10.1046/j.1365-8711.2001.04006.x

Sofue, Y. 2016, Publications of the Astronomical Society of Japan, 68, doi: 10.1093/pasj/psv103

Spergel, D. N., & Steinhardt, P. J. 2000, Phys. Rev. Lett., 84, 3760, doi: 10.1103/PhysRevLett.84.3760

Steigman, G., & Turner, M. S. 1985, Nuclear Physics B, 253, 375, doi: 10.1016/0550-3213(85)90537-1

Taylor, G. I. 1935, Proceedings of the royal society A, 151, 421, doi: 10.1098/rspa.1935.0158

—. 1938, Proceedings of the Royal Society of London Series a-Mathematical and Physical Sciences, 164, 0015, doi: 10.1098/rspa.1938.0002

Xu, Z. 2022a, A comparative study of dark matter flow & hydrodynamic turbulence and its applications, Zenodo, doi: 10.5281/zenodo.6569901

—. 2022b, Dark matter flow dataset Part I: Halo-based statistics from cosmological N-body simulation, Zenodo, doi: 10.5281/zenodo.6541230

—. 2022c, Dark matter flow dataset Part II: Correlation-based statistics from cosmological N-body simulation, Zenodo, doi: 10.5281/zenodo.6569898

—. 2022d, Dark matter flow dataset, 1.0.0, doi: 10.5281/zenodo.6586212